Phase-shift cavity ring-down spectroscopy on a microsphere resonator by Rayleigh backscattering

Jack A. Barnes, Gianluca Gagliardi, and Hans-Peter Loock*
Department of Chemistry, Queen's University, Kingston, Ontario, Canada K7L 3N6
(Received 30 January 2013; published 29 May 2013)

The optical ring-down time in a silica microsphere resonator is measured using phase-shift cavity ring-down spectroscopy. When detecting Rayleigh backscattered light that is coupled into the input waveguide it is found that the shift of the modulation phase angle, $\Delta\phi$, is approximately linearly dependent on the amplitude modulation frequency. The microresonator therefore behaves as if it was a delay line. A model involving two different time scales for the buildup of the Rayleigh backscattered light and the decay of the whispering gallery modes is used to explain the observations.

DOI: 10.1103/PhysRevA.87.053843 PACS number(s): 42.25.Bs, 78.35.+c, 42.79.Gn, 42.25.Fx

Absorption spectroscopy on high-Q microcavities has been proposed as a method to quantify very small quantities of chemicals. Some groups have focused on indirect absorption detection, where the thermal expansion of the cavity upon absorption and the consequent resonance frequency shift have been used as a sensitive indicator [1,2], but this process remains poorly understood [3,4]. Other researchers quantify the optical loss through the decrease in the quality (Q) factor—either by measuring the broadening of the whispering gallery mode (WGM) resonance peaks [5,6] or through a decrease of circulating power and a consequent decrease in transmitted intensity [7,8]. Cavity ring-down (CRD) spectroscopy has also been applied as a convenient and direct determination of optical loss in microcavities [9–14]. In principle one can use CRD spectroscopy in the time domain [9] or use phase-shift measurements [10–12]. The latter technique has the advantages of (1) having a very high duty cycle and (2) enabling measurements of very short ring-down times that are inherent to a microcavity. Phase-shift CRD requires a light source that is modulated at MHz frequencies but does not require fast data acquisition systems.

Microresonators are typically excited by evanescently coupling light from a waveguide structure, such as a tapered optical fiber, into the resonator. To determine cavity ring-down times, light escaping from the microsphere into radiative modes may be collected through a microscope lens or optical fiber [15,16]. For example, Savchenkov *et al.* used this technique to study nonlinear optical effects in a CaF_2 microresonator by monitoring the time-dependent decay of Raman-shifted scattering [14]. Alternatively, one can monitor the intensity of the light traveling through the coupling waveguide [10,17,18]. On resonance this intensity is reduced due to interference between the directly transmitted light and light reemerging from the resonator. Here, we present a third method, which records the frequency, the intensity, and the modulation phase of the Rayleigh backscattered light, i.e., the light that is generated when cavity irregularities invert the direction of propagation and the light is directed back to the laser light source through the waveguide [19]. As will be shown below, the main advantage of this method is the inherent selection for high-Q and high-m whispering gallery modes, a strong background-free signal, and a comparatively simple analysis. We propose that phase-shift CRD measurements of Rayleigh backscattered light provide a viable route to obtain quantitative absorption cross sections of chemical species adsorbed on the microresonator.

In our theoretical models we assume that a single mode is excited. To calculate the phase shift between sinusoidally intensity-modulated light entering and exiting any cavity one can use the Laplace transform of the system's impulse response function, $i(t)$, to calculate the transfer function for the system, $I(s)$ [20–23],

$$I(s) = \mathcal{L}\{i(t)\} = \int_0^\infty e^{-st} i(t)\, dt, \tag{1}$$

where s is a complex frequency given by $s = \sigma + j\omega$ with σ and ω being real and $j = \sqrt{-1}$ [23]. In our application we need only consider imaginary values for s and hence $\sigma = 0$. Here, ω is the angular modulation frequency of the intensity-modulated light [23]. The phase angle, $\phi(\omega)$, of the transfer function can then be obtained from the complex function $I(\omega) = jN(\omega) + D(\omega)$ by noting that $\tan\phi(\omega) = N(\omega)/D(\omega)$. This phase angle equals the phase shift experienced by the sinusoidal input into the cavity. Below we illustrate the procedure by determining phase shifts (a) for light that is scattered from the sphere and collected through a microscope lens and (b) for light that is transmitted through the waveguide; we then discuss (c) light that is Rayleigh backscattered from the sphere.

In a previous article we already described the frequency dependence of the phase angle, ϕ, when the resonant light was *scattered normal to the sphere* [10]. The phase shift is calculated from the Laplace transform of an exponential decay function, i.e., the impulse response of a single-mode decay of a loaded cavity. On resonance,

$$i(t) = A\exp(-t/\tau_L), \tag{2}$$

and the cavity response to an intensity-modulated beam is with Eq. (1),

$$I(\omega) = \frac{A}{\tau_L\left(\omega^2 + 1/\tau_L^2\right)} - j\frac{A\omega}{\left(\omega^2 + 1/\tau_L^2\right)}. \tag{3}$$

The phase shift between the intensity-modulated light entering and exiting the cavity is therefore simply

$$\phi(\omega) = \arctan(-\omega\tau_L). \tag{4}$$

*Corresponding author: hploock@chem.queensu.ca

The ring-down time depends on the optical loss in the cavity with effective length/circumference L and can be calculated from [10]

$$\frac{1}{\tau_L} = \frac{1}{\tau_0} + \frac{1}{\tau_{ex}} \quad \text{with} \quad \tau_{ex} = -\frac{nL}{2c_0 \ln \Gamma}, \tag{5}$$

where c_0 is the speed of light in vacuum, $\sqrt{1-\Gamma^2}$ is the coupling coefficient between the microsphere and taper, and τ_0 is the intensity decay constant (ring-down time) due to absorption and scattering. For a decay involving more modes, we may have a multiexponential decay function and beating in the time domain. The corresponding function for $\tan\phi$ was given by Bescherer *et al.* [20].

The light *transmitted through the taper* experiences a *minimum of intensity* when a WGM resonance is excited and a *maximum of the phase shift* near critical coupling, i.e., when $\tau_0 = \tau_{ex}$ or, equivalently, $nL/c_0\tau_0 = -2\ln\Gamma$. The phase shift is negative in the undercoupled regime, where scattering and absorption losses exceed coupling losses ($nL/c_0\tau_0 > -2\ln\Gamma$), and it is positive in the overcoupled regime where the converse holds ($nL/c_0\tau_0 < -2\ln\Gamma$) [10,11]. The respective equation was derived in [10] and is given as [24]

$$\phi(\omega) = \arctan\left[-\frac{2\omega nL}{c_0}\frac{2\ln\Gamma}{(\ln\Gamma)^2 - (\alpha L/2)^2}\right]. \tag{6}$$

When detecting *Rayleigh backscattered light* the situation is more complicated, since the impulse response function of Eq. (2) is no longer a simple exponential function. In our model the modes of the "forward" circulating light a_f and the backscattered light a_b interconvert at a slow rate given by rate constant k_S, while both modes couple with the same, faster rate given by k_L, to either the taper or to radiative modes, here, both denoted as $[q]$.

$$[a_f] \underset{k_S}{\overset{k_S}{\rightleftarrows}} [a_b]; \quad [a_f] \xrightarrow{k_L} [q]; \quad [a_b] \xrightarrow{k_L} [q]. \tag{7}$$

Mode coupling induced by Rayleigh scattering has been studied by several groups [25–27]. The corresponding differential equations were given by Kippenberg [27,28] as

$$\begin{aligned} \frac{da_f}{dt} &= j\Delta\Omega a_f - \left(\frac{1}{2\tau_0} + \frac{1}{2\tau_{ex}}\right)a_f + \frac{a_b}{2\gamma_{12}} + s(t)\sqrt{1-\Gamma^2}, \\ \frac{da_b}{dt} &= j\Delta\Omega a_b - \left(\frac{1}{2\tau_0} + \frac{1}{2\tau_{ex}}\right)a_b + \frac{a_f}{2\gamma_{21}}. \end{aligned} \tag{8}$$

Here, a_f and a_b are the amplitudes of the mode field. The optical excitation frequency, Ω, is detuned by $\Delta\Omega$ from the whispering gallery mode resonance, the input field amplitude is $s(t)$, and the coupling coefficient between fiber taper and sphere, $1-\Gamma^2 = 1/\tau_{ex}$, is related to the associated decay time. The coefficients describing the interconversion between forward and backward propagated WGMs are imaginary and are related to the Rayleigh backscattering time constant as $\gamma_{12}\gamma_{21} = -\tau_S^2$. The decay rate $k_L = 1/\tau_L = 1/\tau_0 + 1/\tau_{ex}$ depends on the losses through the fiber taper coupler (expressed as τ_{ex}) and on absorption and scattering (τ_0) in the sphere. On resonance $\Delta\Omega = 0$ and the equations in (8) are readily solved using the boundary conditions $a_f(t=0) = 1$, $a_b(t=0) = 0$ and $s(t) = 0$ to give the impulse response function [29],

$$i(t) = |a_b|^2 = \left(\frac{1}{2} - \frac{1}{2}\cos\left[\frac{t}{\tau_S}\right]\right)\exp\left(-\frac{t}{\tau_L}\right). \tag{9}$$

The same result is obtained when $s(t)$ is set to the Dirac delta function $\delta(t)$. For a microresonator the ring-down time due to scattering and absorption $\tau_L = 1/k_L$ can only be shorter than the characteristic scattering time $\tau_S = 1/k_S$ [30]. When $\tau_S \gg \tau_L$ [31,32] the impulse response function of Eq. (9) passes through a maximum at time $t_{max} = 2\tau_L$. The impulse response function also produces a phase angle that is readily derived from Eq. (1) as

$$\tan\phi(\omega) = -\frac{\omega\tau_S^{-2} + 3\omega\tau_L^{-2} - \omega^3}{\tau_L^{-3} - 3\omega^2\tau_L^{-1} + \tau_S^{-2}\tau_L^{-1}}. \tag{10}$$

One can simplify this equation realizing that $\tau_S > \tau_L$ and therefore

$$\tan\phi(\omega) \approx -\frac{\tau_L^3\omega^3 - 3\omega\tau_L}{3\tau_L^2\omega^2 - 1}. \tag{11}$$

In our case this simplification is justified, since we do not observe mode splitting; hence, any splitting given by $1/2\pi\tau_S$ must be much less than the mode linewidth, given by $1/2\pi\tau_L$, here about 13 MHz.

Considering the delayed peak of the impulse response function (9) it is useful to compare the phase-shift response (11) to that of a simple optical delay line of length $L = \tau_L c_0/n$. With Eq. (1) the phase shift of a delay line with impulse response function

$$i(t) = \delta(t - \tau_L) \tag{12}$$

is given by

$$\phi(\omega) = -\omega\tau_L. \tag{13}$$

Note that (11) has a discontinuity at $\omega\tau_L = 3^{-1/2}$; however, the phase shift, $\phi(\omega)$, is continuous as it would be for the delay line of (13). In contrast to a delay line, (11) predicts that $\tan\phi(\omega)$ asymptotically approaches $-3/2\pi$ as ω increases further.

A third impulse response function may be considered a hybrid between (2) and (12). In this approximation we consider the impulse response to be a time-delayed exponential decay, where the delay time and the decay constant are both given by τ_L:

$$\begin{aligned} &i(t) = \exp[-k_L(t - \tau_L)] \quad \text{if } t \geqslant \tau_L, \\ &i(t) = 0 \quad \text{if } t < \tau_L. \end{aligned} \tag{14}$$

For this impulse response function the phase-shift response is a simple sum of (4) and (13):

$$\phi(\omega) = -\omega\tau_L - \arctan(\omega\tau_L). \tag{15}$$

The impulse response functions for all three models, i.e., Eqs. (9), (12), and (14), are shown in Fig. 3(b).

In an experiment one needs to consider an additional phase shift due to light transmission delays, electronic signal delays, delayed detector response, etc. We therefore experimentally determined the offset phase angle by measuring the phase shift from a Fresnel reflection at the end of the fiber containing the taper. We used a fiber taper (diameter 3 μm) to couple light into a silica microsphere (approximate diameter: 300 μm)

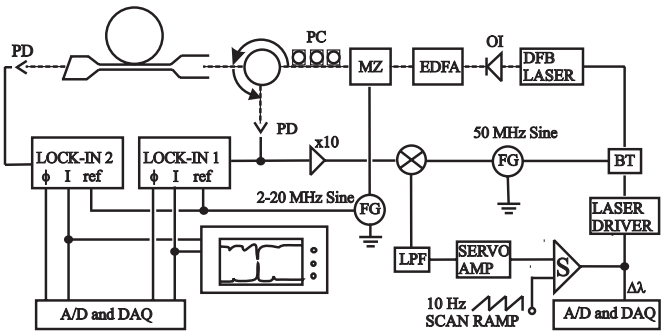

FIG. 1. Setup showing the Pound-Drever-Hall scheme. Distributed feedback laser (DFB); optical isolator (OI); erbium-doped fiber amplifier (EDFA); Mach-Zehnder amplitude modulator (MZ); polarization controller (PC); photodiode (PD); function generator (FG); low-pass filter (LPF); bias-T (BT).

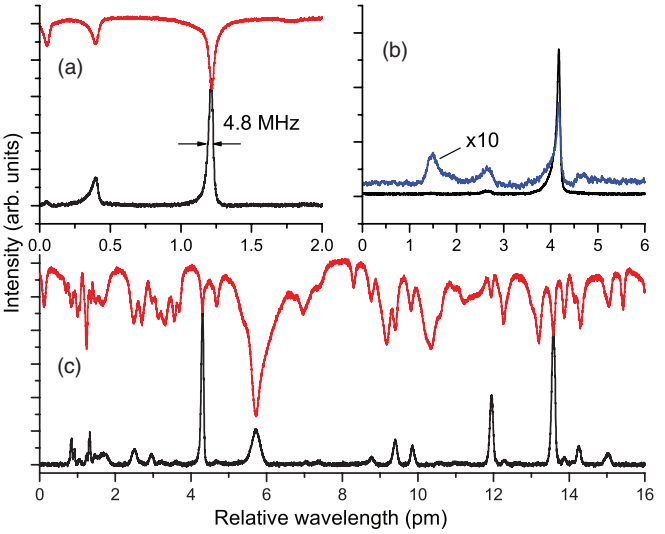

FIG. 2. (Color online) Three different WGM spectra near 1549 nm of a 300-μm silica microsphere (a) obtained by monitoring the transmitted intensity of the fiber taper (red, top) and the Rayleigh backscattered light (black, bottom). A typical isolated resonance (a) has a width of 4.8 MHz corresponding to a Q factor of 42×10^6 and a ring-down time of about 33 ns. (b) A different isolated WGM monitored by recording the scattered intensity through a microscope lens above the sphere ($\times$10, blue) and again through Rayleigh backscatter. (c) shows a larger section of the WGM spectrum. Zero on the relative wavelength scale represents the beginning of the laser scan.

that was fabricated by melting the end of a single-mode fiber (Corning, SMF-28). The sphere was placed under dry nitrogen and light from a distributed feedback (DFB) laser [Avanex 1905LMI, 2-MHz bandwidth (typical), 9 mW, after amplification in an erbium-doped fiber amplifier (EDFA)] was coupled into the sphere. By controlling the polarization of the laser light, TE or TM modes of the microsphere were selectively excited. The WGM spectrum was recorded by placing one detector (Thorlabs DET10C) at the end of the delivery fiber to record transmitted light and a second detector (Thorlabs PDA10CF) after a circulator to record Rayleigh backscattered light (Fig. 1). Light scattered from the microsphere was also recorded by placing a third detector (Thorlabs DET10C) above the microsphere equator, collecting light with a $\times$ 10 microscope objective. The WGM spectra for the transmitted and scattered light were, in general, congested with overlapping modes. The backscattered WGM spectrum was sparser, showing narrower, isolated resonances indicating single, higher-Q-factor modes. This point is illustrated in Fig. 2(c) which compares wide WGM spectral scans recorded in transmission mode and in Rayleigh backscatter mode. Despite the congestion in the transmission and scattering spectra, isolated modes can be observed as is shown in representative spectra of Figs. 2(a) and 2(b). We explain this observation by the bias of Rayleigh backscattered light against low-m modes, and low-Q factors, i.e., only WGMs that "survive" for long enough to build up an appreciable backscattered intensity can be detected, whereas all modes are observed in transmission and scatter. The advantages of detecting Rayleigh backscattered light are particularly apparent when comparing the intensity and width of the WGM spectra to those obtained by collecting scattered light from the sphere using a microscope lens [Fig. 2(b)].

At some of the isolated WGM resonances we measured the phase shift as a function of amplitude modulation frequency. The data were obtained by locking the laser to a sharp, isolated WGM observed through Rayleigh backscatter using the Pound-Drever-Hall method [29,33–35]. While the Pound-Drever-Hall technique requires a MHz frequency modulation (ω_{FM} = 20–50 MHz), we only observed cross talk to the phase-shift measurements ($\omega = \omega_{\mathrm{AM}}$ = 2–20 MHz) when the amplitude modulation fell within a factor of 2 of the frequency modulation. These modulation frequency regimes were therefore avoided.

From Eqs. (10), (13), or (15) we expect to see a continuous response of the phase-shift ϕ when changing the modulation frequency ω. In contrast to all previous phase-shift-CRD experiments, the phase shift can thereby exceed $\pi/2$. Indeed, the experimental data of Fig. 3(a), obtained using a mode which appears intense and isolated when viewed in backscatter, show that the phase shift changes approximately linearly from 0 to approximately -5 rad indicating a behavior that resembles an optical delay line.

A linear fit to Eq. (13) gives $\tau_L = 36$ ns, whereas a fit to Eq. (15) yields $\tau_L = 27$ ns. The "kinetic" model, expressed by (10), produces a fit with $\tau_L = 25$ ns ($Q \approx 30 \times 10^6$), assuming $\tau_S = 100$ ns. This value was estimated as a lower limit based on the lack of mode splitting at a resolution of 10 MHz. On the other hand this model predicts that the phase shift has an asymptotic limit of $-3/2\ \pi$, and the experimental data in Fig. 3(a) do not display this behavior. Indeed in the electronic Supplemental Material [29] we show high-Q modes with $\tau_L = 64$ ns ($Q \approx 78 \times 10^6$) that exhibited phase shifts of -2.7π (–8.5 rad). Figure 3(b) shows the respective impulse response functions for Rayleigh backscattered light that correspond to Eqs. (9), (12), and (14). Of those simple models only Eq. (15) and its corresponding "hybrid" impulse response (14) accurately fit the experimental data, but this impulse response function cannot be derived from the previously published rate equations (8). We suggest that Eq. (14) is an approximation to the result of a more sophisticated model, possibly involving nonlinear effects in the generation of scattering centers in the

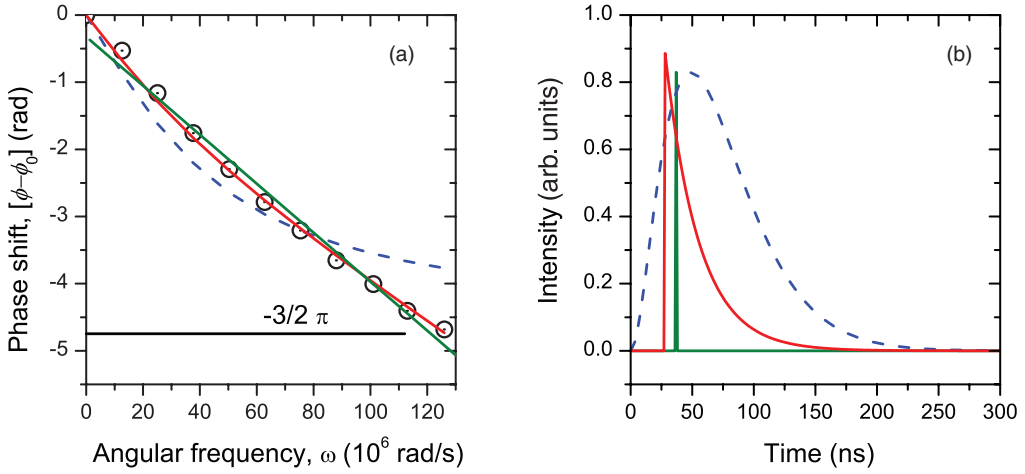

FIG. 3. (Color online) (a) Measured phase shift of the Rayleigh backscattered light as a function of the angular modulation frequency (circles). The solid green line is a linear fit using Eq. (13) with $\tau_L = 36$ ns, the red line uses Eq. (15) with $\tau_L = 27$ ns, and the short-dashed, blue line is a fit to Eq. (11) giving $\tau_L = 25$ ns. (b) Impulse response functions $i(t)$ using the same models and τ_L as in (a), i.e., green line, Eq. (12); red, Eq. (14); and blue, Eq. (9).

microsphere which are not yet included in Eq. (8). Stimulated Brillouin and Raman scattering possess a non-linear gain which could result in an impulse response function similar to Eq. (14) for backscattered light. The backscattered light was therefore examined with a spectrum analyzer. Since the scattered light was not shifted in frequency relative to the input laser light, in our case these non-linear processes can be disregarded as a possible explanation of the observed effect.

It is possible to provide an experimental justification for the use of Eq. (15) in calculating ring-down times for WGMs observed in backscatter. The linewidth of a mode is related to its ring-down time by $\Delta\nu = 1/2\pi\tau$. For an isolated mode, the ring-down time obtained from modulation frequency-dependent phase-shift data, using Eq. (15), can be compared to the value calculated from its measured linewidth. Due to thermal effects, the apparent linewidth of a mode changes with laser power [36]. In determining the linewidth, the EDFA gain was therefore progressively reduced until a constant value for $\Delta\nu$ was achieved (the spectra are not shown here). The linewidth must also be corrected for the instrumental time constant, which causes an asymmetry in the line shape, and for the laser linewidth [16,37]. With these corrections the ring-down time determined from one of the WGM's linewidths is $\tau_L = 10.7$ ns and that calculated using Eq. (15) is $\tau_L = 10.4$ ns ($Q \approx 12 \times 10^6$). Another check can be made by simultaneously obtaining phase-shift data for the same mode but now collecting light that has been scattered from the sphere through a microscope lens. In this case Eq. (4) is expected to describe the phase shift of amplitude-modulated light circulating within a resonator. Figure 4 illustrates that $\tau_L = 10.4$ ns obtained from Rayleigh backscattering agrees very well with the phase-shift data obtained by collecting scattered light above the sphere and with the above linewidth measurement. Of course, to compare ring-down times calculated using scatter and backscatter data, it is necessary to find a mode in the WGM spectrum which shows no overlap with adjacent modes when viewed simultaneously by these two methods.

In conclusion we propose that ring-down spectroscopy on ring cavities can be conducted using Rayleigh-backscattered light. The method is very robust given the minimal effort that is needed to collect the already waveguide-coupled, backscattered light. Furthermore, when collecting Rayleigh backscattered light we observe only those modes that have a long enough lifetime to reverse direction and that furthermore efficiently couple into the waveguide taper, whereas, when detecting scattered light above the sphere, the spectrum is

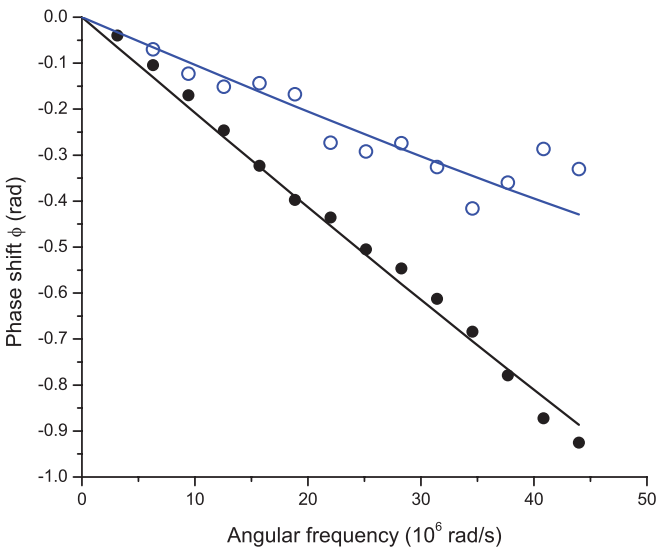

FIG. 4. (Color online) Phase shift observed for a WGM when detecting light scattered tangentially from the sphere (open blue circles) and through Rayleigh backscatter (solid, black circles). The WGM was isolated as in Fig. 2(b). The solid lines are obtained from Eq. (4) (blue line) and Eq. (15) (black line) with $\tau_L = 10.4$ ns in both cases. Due to the high-Q factor of the resonator, the scattering losses are small and the scattering intensity weak, which accounts for the greater noise in the data for the scattering measurement. The apparent, weak oscillation of the data around the fit lines is not understood at present. It may be a coincidence or a sampling artifact.

dominated by WGMs that scatter strongly and therefore have a lower-Q factor. The microsphere spectrum is therefore sparser and dominated by high-Q WGMs when detecting backscattered light. A simple kinetic model predicts the most prominent features of the observed resonance-induced phase shift of intensity-modulated light. The distinguishing feature of the phase-shift measurement on Rayleigh backscattered light is that it appears to be similar to that of an optical delay line with phase shifts that range from 0 to $-\infty$ compared to the range of phase shifts from scattered light detected perpendicular to the sphere (0 to $-\pi/2$) and from that observed through the fiber taper along the "forward" direction ($+\pi/2$ to $-\pi/2$). The optical retardation provided by the microsphere is considerable, especially when considering its size. For example, a value of $\tau_L = 25$ ns (Fig. 3) corresponds to a delay length of 5 m of optical fiber. Data in the electronic Supplemental Material [29] show that a retardation by 64 ns is possible—corresponding to a transmission delay in 12.5 m of optical fiber. Still it should be noted that the most persuasive model, which is based on the impulse response function (9) that was derived from the previously published differential equations (8), cannot quite reproduce the experimental observations, and that a discontinuous "hybrid" impulse response function (14) gives better agreement with our experiments. The source of this discrepancy is presently unknown and more experiments as well as a more thorough analysis of the system may be needed.

The authors thank Saverio Avino for his help in setting up the Pound-Drever-Hall locking scheme. We also thank Queen's University and the Natural Sciences and Engineering Research Council (NSERC) of Canada for funding.

[1] F. Vollmer and S. Arnold, Nat. Methods **5**, 591 (2008).
[2] A. M. Armani, R. P. Kulkarni, S. E. Fraser, R. C. Flagan, and K. J. Vahala, Science **317**, 783 (2007).
[3] A. M. Armani, Science **334**, 1496 (2011).
[4] S. Arnold, S. I. Shopova, and S. Holler, Opt. Express **18**, 281 (2010).
[5] L. Huang and Z. Guo, Nanotechnology **23**, 1 (2012).
[6] A. M. Armani and K. J. Vahala, Opt. Lett. **31**, 1896 (2006).
[7] S. L. Westcott, J. Q. Zhang, R. K. Shelton, N. M. K. Bruce, S. Gupta, S. L. Keen, J. W. Tillman, L. B. Wald, B. N. Strecker, A. T. Rosenberger, R. R. Davidson, W. Chen, K. G. Donovan, and J. V. Hryniewicz, Rev. Sci. Instrum. **79**, 033106 (2008).
[8] G. Farca, S. I. Shopova, and A. T. Rosenberger, Opt. Express **15**, 17443 (2007).
[9] D. K. Armani, T. J. Kippenberg, S. M. Spillane, and K. J. Vahala, Nature **421**, 925 (2003).
[10] J. Barnes, B. Carver, J. M. Fraser, G. Gagliardi, H. P. Loock, Z. Tian, M. W. B. Wilson, S. Yam, and O. Yastrubshak, Opt. Express **16**, 13158 (2008).
[11] H. P. Loock, J. A. Barnes, G. Gagliardi, R. Li, R. D. Oleschuk, and H. Waechter, Can. J. Chem. **88**, 401 (2010).
[12] M. I. Cheema, S. Mehrabani, A. A. Hayat, Y. A. Peter, A. M. Armani, and A. G. Kirk, Opt. Express **20**, 9090 (2012).
[13] M. L. Gorodetsky, A. A. Savchenkov, and V. S. Ilchenko, Opt. Lett. **21**, 453 (1996).
[14] A. A. Savchenkov, A. B. Matsko, M. Mohageg, and L. Maleki, Opt. Lett. **32**, 497 (2007).
[15] K. Grujic, J. P. Hole, O. G. Helleso, and J. S. Wilkinson, Proc. SPIE **6101**, 6101L (2006).
[16] P. Pineda-Vadillo, M. Lynch, C. Charlton, S. Tessarin, J. F. Donegan, and V. Weldon, Electron. Lett. **47**, 129 (2011).
[17] G. C. Righini, Y. Dumeige, P. Feron, M. Ferrari, G. Nunzi Conti, D. Ristic, and S. Soria, Riv. Nuovo Cimento **34**, 435 (2011).
[18] M. S. Luchansky and R. C. Bailey, Anal. Chem. **84**, 793 (2012).
[19] V. Zamora, A. Diez, M. V. Andres, and B. Gimeno, Opt. Lett. **34**, 1039 (2009).
[20] K. Bescherer, J. A. Barnes, S. Dias, G. Gagliardi, H. P. Loock, N. R. Trefiak, H. Waechter, and S. Yam, Appl. Phys. B **96**, 193 (2009).
[21] J. R. Lakowicz, E. Gratton, G. Laczko, H. Cherek, and M. Limkeman, Biophys. J. **46**, 463 (1984).
[22] J. R. Lakowicz, in *Principles of Fluorescence Spectroscopy* (Springer, New York, 2006).
[23] J. DiStefano, A. Stubberud, and I. Williams, *Schaum's Outline of Feedback and Control Systems*, 2nd ed., (McGraw-Hill Education, New York, 2011).
[24] Equation (10) in Ref. [10] is slightly different as it makes a small angle approximation to set $\phi(\omega) = \tan\phi(\omega)$.
[25] D. S. Weiss, V. Sandoghdar, J. Hare, V. Lefevreseguin, J. M. Raimond, and S. Haroche, Opt. Lett. **20**, 1835 (1995).
[26] M. L. Gorodetsky, A. D. Pryamikov, and V. S. Ilchenko, J. Opt. Soc. Am. B **17**, 1051 (2000).
[27] T. J. Kippenberg, S. M. Spillane, and K. J. Vahala, Opt. Lett. **19**, 1669 (2002).
[28] T. J. Kippenberg, Ph.D. dissertation, California Institute of Technology, 2004.
[29] See Supplemental Material at http://link.aps.org/supplemental/10.1103/PhysRevA.87.053843 for details on deriving Eq. (9) and on the Pound-Drever-Hall frequency locking scheme, as well as for additional data on high-Q modes.
[30] J. A. Barnes, H. P. Loock, and G. Gagliardi, in *Cavity Enhanced Spectroscopy and Sensing*, edited by H. P. Loock and G. Gagliardi (Springer, Berlin, 2013).
[31] K. Iwatsuki, K. Hotate, and M. Higashiguchi, Appl. Opt. **23**, 3916 (1984).
[32] M. Nakazawa, J. Opt. Soc. Am. **73**, 1175 (1983).
[33] A. Abramovici, W. E. Althouse, R. W. P. Drever, Y. Gursel, S. Kawamura, F. J. Raab, D. Shoemaker, L. Sievers, R. E. Spero, K. S. Thorne, R. E. Vogt, R. Weiss, S. E. Whitcomb, and M. E. Zucker, Science **256**, 325 (1992).
[34] E. D. Black, Am. J. Phys. **69**, 79 (2001).
[35] S. Avino, J. A. Barnes, G. Gagliardi, X. J. Gu, D. Gutstein, J. R. Mester, C. Nicholaou, and H. P. Loock, Opt. Express **19**, 25057 (2011).
[36] C. Schmidt, A. Chipouline, T. Pertsch, A. Tunnermann, O. Egorov, F. Lederer, and L. Deych, Opt. Express **16**, 6285 (2008).
[37] G. J. Butterworth, J. Phys. E **1**, 1165 (1968).